

Spectroscopy of Doubly-Charmed Baryons in Lattice QCD

UKQCD Collaboration

J.M. Flynn, F. Mescia and A.S.B. Tariq

*Department of Physics and Astronomy, University of Southampton,
Southampton, SO17 1BJ, United Kingdom.*

Abstract

We present results for masses of spin-1/2 and spin-3/2 double-charm baryons in quenched lattice QCD, from an exploratory study using a non-perturbatively improved clover action at $\beta = 6.2$. We have studied local operators and we observe, after appropriate projections, a good signal for the ground states. We also present results for single-charmed baryons and spin-splittings for both double- and single-charmed states.

1 Introduction

Recently SELEX, the charm hadroproduction experiment at Fermilab, has reported a narrow state at $3519 \pm 1 \pm 5$ MeV. This state decays into $\Lambda_c^+ K^- \pi^+$, consistent with the weak decay of the doubly charmed baryon Ξ_{cc}^+ [1]. This is the first observation of a baryon containing two charm quarks. BaBar and Belle at the SLAC and KEK b -factories may also provide further evidence of doubly charmed baryons.

Double charmed baryons combine the opposites of the slow relative motion of two heavy quarks with the fast motion of a light quark. They provide scope for testing ideas developed for single charm physics, such as the predicted hierarchies in lifetimes and semi-leptonic branching ratios and give us more room to explore predictions of exotic tetra- and penta-quark states (see the review by Richard [2] for further details). Unresolved issues regarding the recent SELEX observation itself include the fact that the observed lifetime of less than 30 fs is much less than predicted by quark models [3] and that the observed isospin splitting $m(ccd) - m(ccu)$ is rather large, about 60 times that for nucleons. The latter is, perhaps, the cause for publication of only one of the three states (the others being around 3460 and 3780 MeV) observed in the first instance (see e.g. [4]). Therefore it is important to study these baryons further.

The first prediction for the masses of these double-charmed baryons comes from the early work of De Rujula *et al.* [5], with later calculations from quark models and QCD sum rules [6–15].

Lattice QCD provides a method of calculating the masses of these baryons from first principles in a model-independent and non-perturbative manner. It is interesting to compare the results from different lattice calculational techniques. Previous lattice calculations have used the D234 action [16] and NRQCD [17]. NRQCD is less suitable for charm quarks than for beauty quarks, and furthermore charm quark masses are very accessible to lattice simulation without using an effective theory. In this calculation we use a non-perturbatively $\mathcal{O}(a)$ -improved clover action [18]. Thus our results have discretisation errors $\mathcal{O}(m_q^2 a^2)$, with $m_q^2 a^2$ about 25% in our simulation. Interestingly, although our double-charm baryons have masses larger than one in lattice units, the physical mass looks consistent for the one state for which an experimental number is available.

We also study spin-splittings for charmed baryons and mesons, where the leading charm quark mass dependence cancels. Recent calculations using the $\mathcal{O}(a)$ non-perturbatively improved clover action find vector-pseudoscalar meson splittings in better agreement [19, 20] with experiment than earlier calculations using less-improved clover actions [21]. We confirm this here. For the single-charmed baryons, calculations with a tree-level clover action had difficulty reproducing the experimental splittings [22], while simulations using the D234 [16] or NRQCD [17] actions were compatible with experiment. We too find compatibility. For the doubly-charmed baryons, experimental data are not yet available. However, our results are compatible with those from the D234 and NRQCD actions. Since the hyperfine splitting is sensitive to the chromomagnetic moment term in the improved clover fermion action, we believe this shows the importance of using the non-perturbative value for its coefficient (c_{SW}). A similar observation was made concerning the coupling

Baryon	Quark content	Mass [MeV]
Ξ_{cc}	$\frac{s_{cc} = 1, J^P = 1/2^+}{ccu, ccd}$	3519(5)
Ω_{cc}	ccs	
Ξ_{cc}^*	$\frac{s_{cc} = 1, J^P = 3/2^+}{ccu, ccd}$	
Ω_{cc}^*	ccs	
Λ_c	$\frac{s_{ll} = 0, J^P = 1/2^+}{cud}$	2285(1)
Ξ_c	cus, cds	2469(1)
Σ_c	$\frac{s_{ll} = 1, J^P = 1/2^+}{cuu, cud, cdd}$	2452(1)
Ξ_c'	cus, cds	2575(3)
Ω_c	css	2698(3)
Σ_c^*	$\frac{s_{ll} = 1, J^P = 3/2^+}{cuu, cud, cdd}$	2518(2)
Ξ_c^*	cus, cds	2646(2)
Ω_c^*	css	

Table 1. Summary of charmed baryons. Valence quark content and spin-parity are shown. The quantities s_{cc} and s_{ll} are the total spin of the charm and light quark pair respectively. The experimental values are from ref. [23], averaged over isospin multiplets. The Ξ_{cc} mass is from the recent observation of the $\Xi_{cc}^+(ccd)$ [1].

with the chromomagnetic field in the NRQCD action [17] (c_4 in eq. (A5) in [17]).

Our final results for the double-charm masses and splittings are

$$\begin{aligned}
\Xi_{cc} &= 3549(13)(19)(92) \text{ MeV} & \Omega_{cc} &= 3663(11)(17)(95) \text{ MeV} \\
\Xi_{cc}^* &= 3641(18)(8)(95) \text{ MeV} & \Omega_{cc}^* &= 3734(14)(8)(97) \text{ MeV} \\
\Xi_{cc}^* - \Xi_{cc} &= 87(13)(13)(2) \text{ MeV} & \Omega_{cc}^* - \Omega_{cc} &= 67(9)(13)(2) \text{ MeV}
\end{aligned} \tag{1}$$

The splittings are determined by fitting ratios of correlators, which gives smaller errors compared to taking a difference of separately-fitted masses. Results for charmed meson splittings and single-charm baryon masses and splittings are in the body of the paper.

In this paper the theoretical input and computational details of the simulation are given in Sections 2 and 3, whereas the results are presented and analysed in Section 4. There is a brief conclusion in Section 5.

2 Baryon states and interpolating operators

The double and single charmed baryons expected in QCD are summarised in tab. 1.

On the lattice, the masses of these hadrons can be calculated in the usual way from

the large time behaviour of two point correlation functions

$$C(t) = \sum_{\mathbf{x}} \langle 0 | J(\mathbf{x}, t) \bar{J}(0) | 0 \rangle \quad (2)$$

where the J 's are interpolating operators with quantum numbers to create or annihilate the state of interest. The choice of operators is not unique.

For the spin-1/2 doubly-heavy baryon states, a simple operator is

$$J_\gamma = \epsilon_{abc} h_\gamma^a \left(h^{bT} \gamma_5 \mathcal{C} l^c \right), \quad s_{hh} = 1 \quad (3)$$

where a, b, c are colour indices, \mathcal{C} is the charge conjugation matrix and the h and l fields stand for generic heavy and light quarks.

In S -wave baryons with two identical quarks (heavy quarks in our case), the two quarks cannot couple to spin zero and the only possibility is $s_{hh} = 1$ (symmetric in both spin and flavour). The component $s_{hh} = 0$ as well as the operator $-\epsilon_{abc} l_\gamma^a (h^{bT} \gamma_5 \mathcal{C} h^c)$ vanish. The coupling of the light-quark spin to $s_{hh} = 1$, however, can also generate the spin 3/2 states, Ξ_{hh}^* and Ω_{hh}^* in tab. 1.

An interpolating operator for the spin-3/2 states can be obtained by replacing γ_5 with γ^μ in eq. (3).

$$J_\gamma^\mu = \epsilon_{abc} h_\gamma^a \left(h^{bT} \gamma^\mu \mathcal{C} l^c \right), \quad s_{hh} = 1. \quad (4)$$

This operator also couples to spin-1/2 and projections are needed to obtain the desired state. The spin-1/2 masses from J_γ^μ and J_γ are equal since there is only one spin 1/2 baryon in the situation where two quarks are identical. We have directly verified this property in our simulation.

Another operator, used for spin-3/2 double heavy baryons [17, 24] is

$$\tilde{J}_\gamma^\mu = \epsilon_{abc} l_\gamma^c (h^{bT} \gamma^\mu \mathcal{C} h^a). \quad (5)$$

We have also tried this operator and we see no reason to prefer one over the other. Indeed, both give a good overlap for the ground state and the masses extracted turn out to be equal as expected.

For the operators J_γ and J_γ^μ (or \tilde{J}_γ^μ) the 2-point functions in eq. (2) have the following large-time behaviour

$$\begin{aligned} C(t)_{\gamma\bar{\gamma}} &= \sum_{\mathbf{x}} \langle 0 | J_\gamma(\mathbf{x}, t) \bar{J}_{\bar{\gamma}}(0) | 0 \rangle \\ &\xrightarrow{t \gg 0} Z_{1/2} (P_+)_{\gamma\bar{\gamma}} e^{-m_{1/2} t} + Z_{1/2}^P (P_-)_{\gamma\bar{\gamma}} e^{-m_{1/2}^P t}. \end{aligned} \quad (6)$$

$$\begin{aligned} C_2(t)_{\gamma\bar{\gamma}}^{ij} &= \sum_{\mathbf{x}} \langle 0 | J_\gamma^i(\mathbf{x}, t) \bar{J}_{\bar{\gamma}}^j(0) | 0 \rangle \\ &\xrightarrow{t \gg 0} Z_{3/2} \left(P_+ P_{3/2}^{ij} \right)_{\gamma\bar{\gamma}} e^{-m_{3/2} t} + Z_{1/2} \left(P_+ P_{1/2}^{ij} \right)_{\gamma\bar{\gamma}} e^{-m_{1/2} t} \\ &\quad + Z_{3/2}^P \left(P_- P_{3/2}^{ij} \right)_{\gamma\bar{\gamma}} e^{-m_{3/2}^P t} + Z_{1/2}^P \left(P_- P_{1/2}^{ij} \right)_{\gamma\bar{\gamma}} e^{-m_{1/2}^P t} \end{aligned} \quad (7)$$

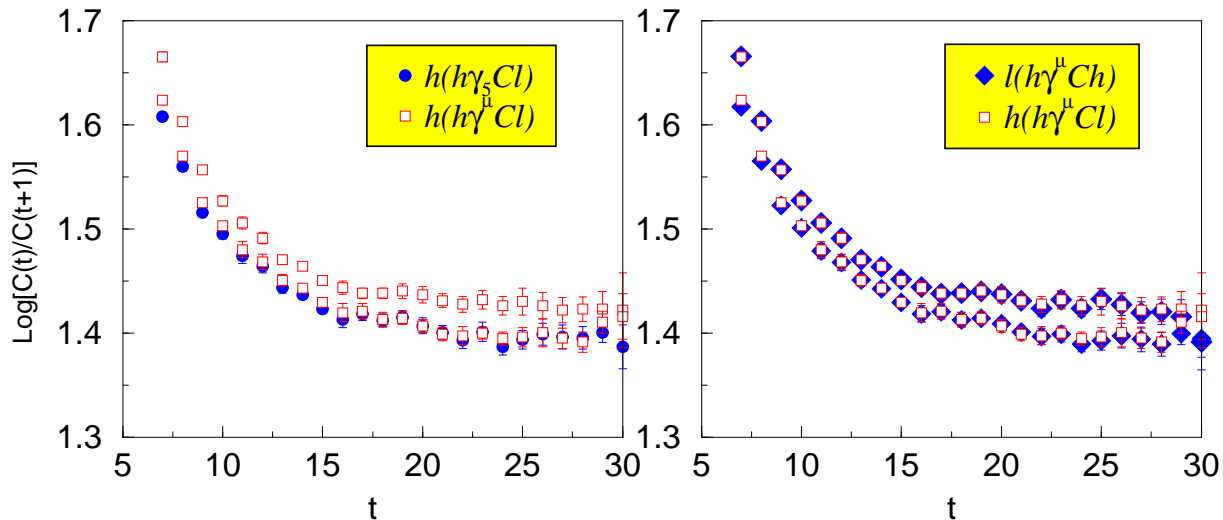


Figure 1. Comparison of the effective mass plots for the double heavy operators J_γ , J_γ^μ and \tilde{J}_γ^μ , with $\kappa_h = 0.1222$ and $\kappa_l = 0.1351$. In each plot the upper points are for spin-3/2 and the lower points for spin-1/2. The spin-1/2 plateaus are the same for J_γ and J_γ^μ (left) while both plateaus coincide for the J_γ^μ and \tilde{J}_γ^μ operators (right).

where the projection operators are defined by

$$\begin{aligned}
 P_- &= \frac{1 + \gamma_0}{2}, & P_+ &= \frac{1 - \gamma_0}{2}, \\
 P_{3/2}^{ij} &= g^{ij} - \frac{1}{3}\gamma^i \gamma^j, & P_{1/2}^{ij} &= \frac{1}{3}\gamma^i \gamma^j.
 \end{aligned}
 \tag{8}$$

Contributions of negative parity states are removed by projection with P_+ . The negative parity states can, in principle, be detected by using the projector P_- , but in our simulation they are much noisier. We show an example of the signals from the operators J_γ , J_γ^μ and \tilde{J}_γ^μ in fig. 1. As stressed above, spin-1/2 masses extracted using the three operators are equal, while the choice between J_γ^μ and \tilde{J}_γ^μ makes no difference for the spin-3/2 mass.

For a baryon containing a single heavy quark, a common choice of operators is

$$\mathcal{O}_\gamma = \epsilon_{abc} h_\gamma^a \left(l_1^{bT} \gamma_5 \mathcal{C} l_2^c \right), \quad s_{ll} = 0, \tag{9}$$

$$\mathcal{O}_\gamma^\mu = \epsilon_{abc} h_\gamma^a \left(l_1^{bT} \gamma^\mu \mathcal{C} l_2^c \right), \quad s_{ll} = 1, \tag{10}$$

for the states $s_{ll} = 0$ and $s_{ll} = 1$ in tab. 1, respectively. In our simulation, the light quarks l_1, l_2 carry different flavours but the same masses.

κ_l	am_P	am_V
0.1344	0.300(2)	0.397(4)
0.1346	0.276(2)	0.383(5)
0.1351	0.210(3)	0.352(11)
0.1353	0.177(2)	0.340(15)

Table 2. Light pseudoscalar and vector meson masses. The fit interval is [12 – 28]. Our time counting starts from 0.

It should be noted that for baryons three different quarks, i.e., hl_1l_2 (or lh_1h_2), these two operators correspond to different physical spin-1/2 states with $s_{ll} = 0$ and 1 respectively, the latter one often being denoted by a prime. This is evident from the experimental masses of Ξ_c and Ξ'_c in tab. 1.

3 Details of the Simulation

Our simulation was made using the code FermiQCD [25] on a PC cluster. In this study 100 quenched gauge configurations were generated at $\beta = 6.2$ on a volume of $24^3 \times 64$ with 1000 heatbath steps for the thermalisation followed by 200 heatbath steps to separate each gauge configuration. These numbers were decided upon after an autocorrelation study on the average plaquette values.

Four light quark propagators around the strange quark mass and three heavy quark propagators around the charm were calculated using the following values of the hopping parameters:

- $\kappa_l = 0.1344, 0.1346, 0.1351, 0.1353$;
- $\kappa_h = 0.1240, 0.1233, 0.1222$.

The propagators were generated by the Bistabilised Conjugate Gradient method [26] for the non-perturbatively improved clover action [18].

Since the signal is satisfactory with local interpolating operators, no smearing was required. The statistical errors were estimated by a jackknife procedure, removing 10 configurations at a time from the ensemble.

3.1 Lattice spacing and quark masses

To fix the lattice spacing, we used the *method of lattice planes* [27]. In other words, we perform the following fit to the light vector and pseudoscalar masses in table 2,

$$am_V = C + L(am_P)^2. \quad (11)$$

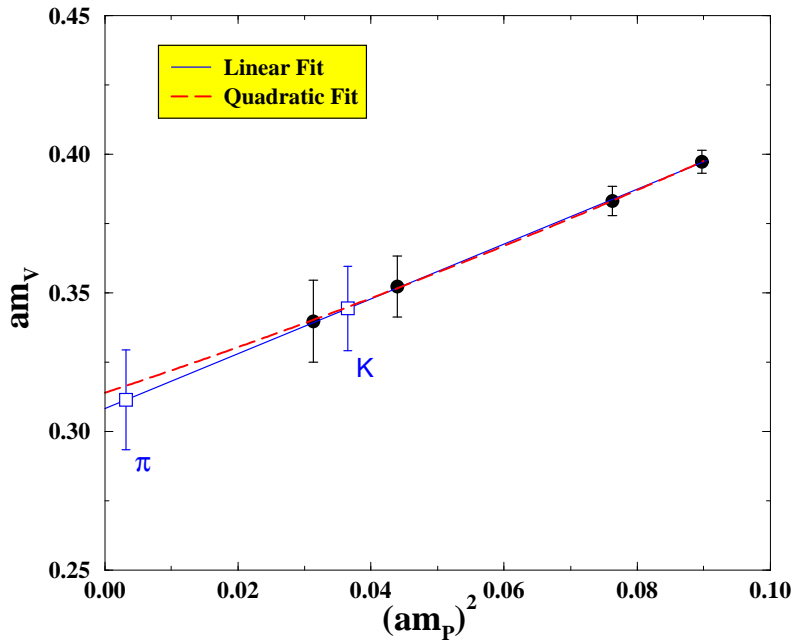


Figure 2. Light vector masses as a function of squared light pseudoscalar masses. The interpolated kaon and extrapolated pion masses are also shown.

This is shown in fig. 2. From the physical values of m_{K^*} and m_K , the inverse lattice spacing is found to be

$$a^{-1} = 2.6(1) \text{ GeV}. \quad (12)$$

Terms of $\mathcal{O}((am_P)^4)$ in eq. (11) turn out to be irrelevant and do not affect the above estimate (compare the linear and quadratic fits in fig. 2). For illustration, the values of the pseudoscalar masses in tab. 2 converted to physical units are

$$m_P = \{779, 716, 546, 459\} \text{ MeV}. \quad (13)$$

These span the kaon mass while the pion is instead quite far away. For this reason, we interpolate for the strange quark and extrapolate for the up/down masses. This is also the reason for using K, K^* to fix the lattice spacing.

For the heavy sector, the D_s -meson mass is within our range of simulation. This is evident once the heavy-light pseudoscalar masses in tab. 3 are interpolated to the strange mass (through the lattice plane method) and expressed in physical units

$$m_{h,s} = \{1.83, 1.89, 1.98\} \text{ GeV}. \quad (14)$$

$\kappa_h - \kappa_l$	am_P	$am_{hll'}$			am_{hhl}	
		$J^P = \frac{1}{2}^+$ $s_{ll'} = 0$	$J^P = \frac{1}{2}^+$ $s_{ll'} = 1$	$J^P = \frac{3}{2}^+$ $s_{ll'} = 1$	$J^P = \frac{1}{2}^+$ $s_{hh} = 1$	$J^P = \frac{3}{2}^+$ $s_{hh} = 1$
0.1240-0.1344	0.718(2)	0.954(5)	0.988(6)	1.008(6)	1.326(3)	1.354(3)
0.1233-0.1344	0.740(2)	0.975(5)	1.010(6)	1.029(6)	1.368(3)	1.395(3)
0.1222-0.1344	0.775(2)	1.008(6)	1.044(6)	1.062(6)	1.433(3)	1.459(3)
$\kappa_{\text{charm}}-0.1344$		1.003(28)	1.039(33)	1.057(32)	1.055(31)	1.442(57)
0.1240-0.1346	0.710(2)	0.934(6)	0.972(7)	0.992(7)	1.318(4)	1.347(4)
0.1233-0.1346	0.733(2)	0.956(6)	0.994(7)	1.013(7)	1.360(4)	1.388(3)
0.1222-0.1346	0.767(2)	0.989(6)	1.028(7)	1.046(7)	1.425(3)	1.452(3)
$\kappa_{\text{charm}}-0.1346$		0.984(28)	1.023(34)	1.041(33)	1.416(57)	1.442(57)
0.1240-0.1351	0.691(3)	0.878(10)	0.929(13)	0.945(10)	1.297(4)	1.329(5)
0.1233-0.1351	0.714(3)	0.900(10)	0.951(13)	0.966(10)	1.339(5)	1.370(5)
0.1222-0.1351	0.748(3)	0.934(10)	0.984(14)	0.998(10)	1.404(5)	1.434(5)
$\kappa_{\text{charm}}-0.1351$		0.928(27)	0.979(39)	0.993(34)	1.395(58)	1.425(58)
0.1240-0.1353	0.683(3)	0.854(13)	0.903(17)	0.915(12)	1.287(5)	1.322(6)
0.1233-0.1353	0.706(3)	0.876(13)	0.923(17)	0.935(12)	1.330(5)	1.363(6)
0.1222-0.1353	0.740(3)	0.910(13)	0.956(18)	0.967(12)	1.395(6)	1.427(6)
$\kappa_{\text{charm}}-0.1353$		0.904(28)	0.951(43)	0.962(34)	1.385(58)	1.418(58)

Table 3. Double and single-heavy baryon masses in lattice units, together with pseudoscalar masses. The fit intervals are [16 – 28] for double and [15 – 25] for single-heavy baryons.

3.2 Analysis of the baryon masses

Since κ_{charm} is rather close to our third $\kappa_h = 0.1222^1$, as the first step in our analysis, we interpolate the quantities of interest, *viz.* the single and double heavy baryon masses, to the charm mass. In practice, this procedure is implemented by doing for each κ_l the following fits

$$am_{hhl} = C_l + L_l am_{hs}, \quad am_{hll} = C'_l + L'_l am_{hs}. \quad (15)$$

Quantities at the charm mass, m_{ccl} and m_{cll} are obtained by putting $m_{hs} = m_{D_s}$. This interpolation is shown for the double heavy case in fig. 3. With the charm mass fixed, the

¹A naive linear fit in $1/\kappa_h$ to the masses in eq. (14) gives $\kappa_{\text{charm}} = 0.1224(9)$.

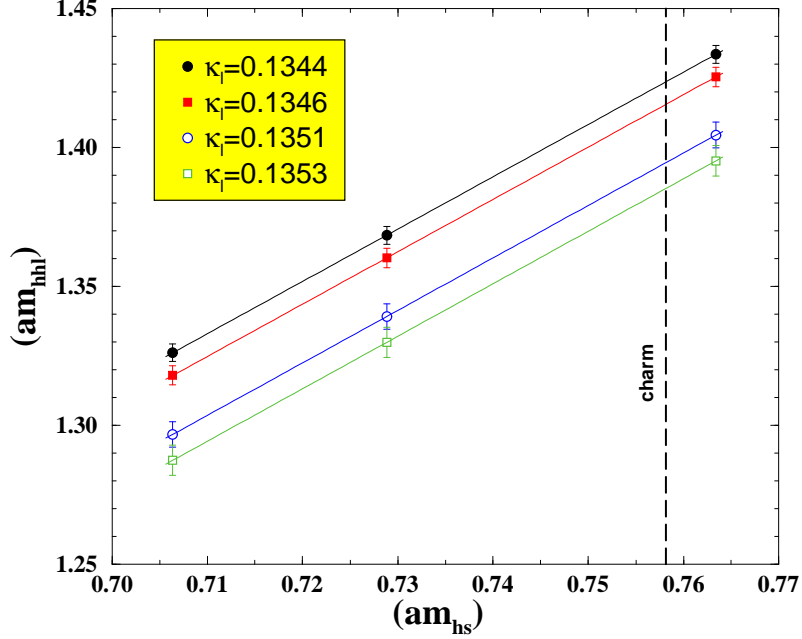


Figure 3. Spin-1/2 double-heavy baryon masses for all κ combinations. For each κ_l we fit the heavy quark mass dependence using the heavy-strange pseudoscalar meson mass. The fit function is given in equation (15). The vertical dashed line indicates the D_s meson mass (in lattice units) used to fix the masses of the ccl spin-1/2 baryons.

light quark mass dependence is studied using

$$am_{ccl} = A + B(am_P)^2, \quad am_{ccl} = A' + B'(am_P)^2. \quad (16)$$

This fit is shown for the spin-1/2 double charm case in fig. 4. The masses of charmed baryons containing strange and/or up/down quarks are obtained by the following substitutions for m_P in the above equations:

- $m_P = m_\pi$ for m_{cud} , m_{ccu} ;
- $m_P = m_K$ for m_{csu} ;
- $m_P = m_{\eta_{ss}}$ for m_{css} , m_{ccs} .

where $m_{\eta_{ss}}^2 = 2m_K^2 - m_\pi^2$. In the second case, we suppose that $SU(3)$ breaking terms are negligible and obtain our estimate from states containing two mass-degenerate light quarks [24, 27].

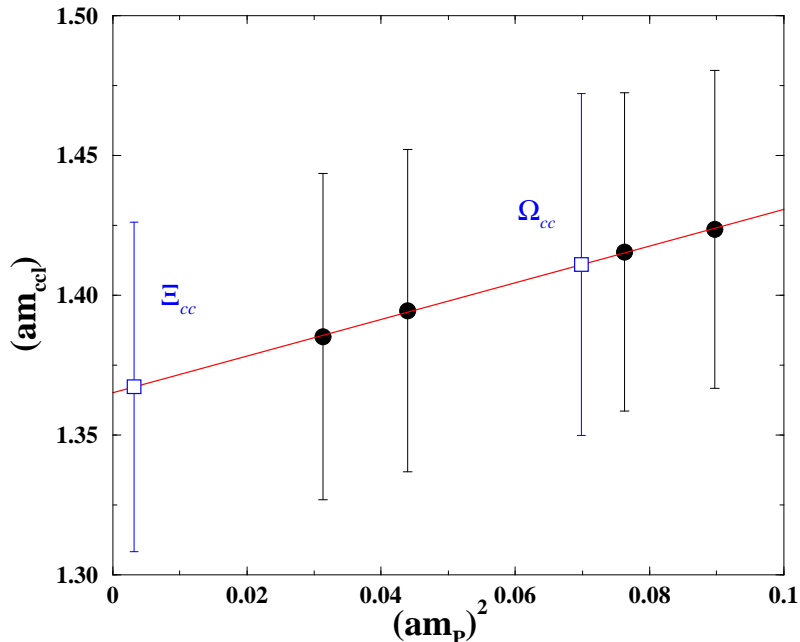


Figure 4. Spin-1/2 double charm state masses as a function of the square of the light pseudoscalar masses. The values at strange and up/down masses are shown.

4 Results and Discussion

Here we recall our final values for the double-charm baryon masses.

$$\begin{aligned}
 \Xi_{cc} &= 3549(13)(19)(92) \text{ MeV} & \Omega_{cc} &= 3663(11)(17)(95) \text{ MeV} \\
 \Xi_{cc}^* &= 3641(18)(8)(95) \text{ MeV} & \Omega_{cc}^* &= 3734(14)(8)(97) \text{ MeV}
 \end{aligned}
 \tag{17}$$

The first error is statistical. The second error is systematic, estimated by combining in quadrature the effects of the following variations in our analysis:

- changing the time fit-ranges — this contributes up to 35% of the quoted error;
- using single or double exponential fits — we saw no change in our lowest state masses;
- linear versus quadratic chiral extrapolations — in the worst case this gives three-quarters of the quoted error;
- interchanging the order of light quark extrapolations and charm quark interpolation — this produces no change in our results.

Only one volume and lattice spacing was studied; investigation of discretization errors, the continuum limit and finite volume effects are not addressed. To account for these (and the effects of quenching), the third quoted error is found by rescaling our masses using the experimental Λ_c mass.

	This work [MeV]	Expt [MeV]
Λ_c	2227(50)(57)(58)	2285(1)
Ξ_c	2374(34)(23)(61)	2469(1)
Σ_c	2377(38)(84)(62)	2452(1)
Ξ'_c	2502(26)(40)(65)	2575(3)
Ω_c	2627(16)(48)(68)	2698(3)
Σ_c^*	2396(42)(122)(62)	2518(2)
Ξ_c^*	2532(31)(62)(66)	2646(2)
Ω_c^*	2669(21)(26)(70)	

Table 4. Our estimates for the single charm baryon masses compared to experimental values.

The Ξ_{cc} mass is in good agreement with the experimental value [1]

$$(\Xi_{cc})_{\text{expt}} = 3519 \pm 1 \pm 5 \text{ MeV} \quad (18)$$

Other masses are consistent with the lattice estimates using NRQCD [17] or D234 [16] actions. For recent estimates in quark models or QCD Sum Rules we refer the reader to [15] and [13] respectively. For completeness, our estimates for the single charm baryon masses are given in tab. 4 along with the experimental results. Values turn out to be compatible with previous lattice calculations [17, 22, 24]. It may be noted that in ref. [22], a perturbative value for the coefficient c_{SW} was used in the clover action.

We now turn to the baryon and meson spin-splittings. Our results for these are given in tab. 5. The values are obtained either from the difference in individually fitted masses (labelled “Diff” in the table), or by directly fitting a ratio of correlators (labelled “Ratio” in the table). When using the ratio the noise starts to dominate earlier so we restrict our fit to a shorter time-slice window. For the baryons we find a better signal using the ratio method and the difference between the two approaches becomes more apparent as we move away from our region of simulation to lighter quarks. We use the numbers from the ratio as our best estimates.

For the double-charm baryons we observe a good signal for non-zero splittings. For the single-charm baryons, where experimental data is available, our results are compatible. This distinguishes our results from earlier ones using a less-improved clover action [22]. Our values are also compatible with those found using the D234 [16] or NRQCD [17] actions. For the mesons too our results are compatible with experiment: this improved agreement is also found in other recent non-perturbatively improved clover simulations [19, 20].

The predictions are more precise for (Ω_c^*, Ω_c) and the double charm spin doublets $(\Omega_{cc}^*, \Omega_{cc})$ and (Ξ_{cc}^*, Ξ_{cc}) , where less extrapolation is needed, but experimental numbers are still awaited.

	Diff [MeV]	Ratio [MeV]	Expt [MeV]
$\Xi_{cc}^* - \Xi_{cc}$	89(15)	87(13)(13)(2)	
$\Omega_{cc}^* - \Omega_{cc}$	69(10)	67(9)(13)(2)	
$\Sigma_c^* - \Sigma_c$	18(51)	49(39)(12)(1)	66(2)
$\Xi_c^* - \Xi_c'$	30(33)	47(27)(4)(1)	71(3)
$\Omega_c^* - \Omega_c$	43(17)	44(16)(15)(1)	
$D^* - D$		127(14)(1)(3)	142(2)
$D_s^* - D_s$		123(11)(1)(3)	138(2)

Table 5. Our results for the single- and double-charm mass splittings.

5 Conclusion

We have presented exploratory quenched lattice results for double charm baryon masses. These have drawn attention after the experimental observation of the first double charm state last year. The calculation is done with non-perturbatively $\mathcal{O}(a)$ -improved Wilson fermions at $\beta = 6.2$ and on a large lattice. Good signals for the ground states are observed without recourse to smearing. In addition, we have reported the masses of single charm baryons. The calculated masses look quite reasonable. We see a definite signal for non-zero baryon and meson spin splittings. To improve our lattice calculations, a finer lattice spacing is necessary together with an examination of chiral logarithms in the light extrapolations and a simulation with dynamical quarks.

Experimental observations of the remaining double charmed baryon states and, in particular their spin-splittings, would allow the lattice predictions to be checked.

Acknowledgments

We would like to thank Massimo Di Pierro for his help in using the FermiQCD code. We also thank the Iridis parallel computing team at University of Southampton, in particular, Ivan Wolton, Ian Hardy and Oz Parchment for their computing support. We thank Craig McNeile and Chris Maynard for useful discussions and cross-checks; Damir Becirevic, Andreas Kronfeld, Vittorio Lubicz and Cecilia Tarantino for comments. The work of ASBT is supported by a Commonwealth Scholarship. Work partially supported by the European Community's Human Potential Programme under HPRN-CT-2000-00145 Hadrons/Lattice QCD.

References

- [1] M. Mattson *et al.* [SELEX Collaboration], Phys. Rev. Lett. **89**, 112001 (2002) [arXiv:hep-ex/0208014].
- [2] J. M. Richard, arXiv:hep-ph/0212224.
- [3] V. V. Kiselev and A. K. Likhoded, arXiv:hep-ph/0208231.
- [4] M. A. Moinester *et al.* [SELEX Collaboration], arXiv:hep-ex/0212029.
- [5] A. De Rujula, H. Georgi and S. L. Glashow, Phys. Rev. D **12** (1975) 147.
- [6] S. Fleck and J. M. Richard, Prog. Theor. Phys. **82** (1989) 760.
- [7] M. J. Savage and M. B. Wise, Phys. Lett. B **248** (1990) 177.
- [8] E. Bagan, H. G. Dosch, P. Gosdzinsky, S. Narison and J. M. Richard, Z. Phys. C **64** (1994) 57 [arXiv:hep-ph/9403208].
- [9] R. Roncaglia, D. B. Lichtenberg and E. Predazzi, Phys. Rev. D **52** (1995) 1722 [arXiv:hep-ph/9502251].
- [10] S. S. Gershtein, V. V. Kiselev, A. K. Likhoded and A. I. Onishchenko, Mod. Phys. Lett. A **14** (1999) 135 [arXiv:hep-ph/9807375].
- [11] S. P. Tong, Y. B. Ding, X. H. Guo, H. Y. Jin, X. Q. Li, P. N. Shen and R. Zhang, Phys. Rev. D **62** (2000) 054024 [arXiv:hep-ph/9910259].
- [12] D. Ebert, R. N. Faustov, V. O. Galkin and A. P. Martynenko, Phys. Rev. D **66** (2002) 014008 [arXiv:hep-ph/0201217].
- [13] V. V. Kiselev and A. E. Kovalsky, Phys. Rev. D **64** (2001) 014002 [arXiv:hep-ph/0005019].
- [14] I. M. Narodetskii and M. A. Trusov, arXiv:hep-ph/0209044.
- [15] I. M. Narodetskii, A. N. Plekhanov and A. I. Veselov, JETP Lett. **77** (2003) 58 [Pisma Zh. Eksp. Teor. Fiz. **77** (2003) 64] [arXiv:hep-ph/0212358].
- [16] R. Lewis, N. Mathur and R. M. Woloshyn, Phys. Rev. D **64**, 094509 (2001) [arXiv:hep-ph/0107037].
- [17] N. Mathur, R. Lewis and R. M. Woloshyn, Phys. Rev. D **66** (2002) 014502 [arXiv:hep-ph/0203253].
- [18] M. Luscher, S. Sint, R. Sommer, P. Weisz and U. Wolff, Nucl. Phys. B **491** (1997) 323 [arXiv:hep-lat/9609035].

- [19] K. C. Bowler, L. Del Debbio, J. M. Flynn, G. N. Lacagnina, V. I. Lesk, C. M. Maynard and D. G. Richards [UKQCD Collaboration], Nucl. Phys. B **619** (2001) 507 [arXiv:hep-lat/0007020].
- [20] D. Becirevic, P. Boucaud, J. P. Leroy, V. Lubicz, G. Martinelli, F. Mescia and F. Rapuano, Phys. Rev. D **60** (1999) 074501 [arXiv:hep-lat/9811003].
- [21] C. R. Allton *et al.* [UKQCD Collaboration], Phys. Lett. B **292** (1992) 408 [arXiv:hep-lat/9208018].
- [22] K. C. Bowler *et al.* [UKQCD Collaboration], Phys. Rev. D **54** (1996) 3619 [arXiv:hep-lat/9601022].
- [23] K. Hagiwara *et al.* [Particle Data Group], Phys. Rev. D **66**, 010001 (2002) and 2003 off-year partial update for the 2004 edition available on the PDG WWW pages (URL: <http://pdg.lbl.gov/>)
- [24] A. Ali Khan *et al.*, Phys. Rev. D **62** (2000) 054505 [arXiv:hep-lat/9912034].
- [25] M. Di Pierro, Nucl. Phys. Proc. Suppl. **106** (2002) 1034 [arXiv:hep-lat/0110116]; M. Di Pierro, arXiv:hep-lat/0011083.
- [26] A. Frommer, V. Hannemann, B. Nockel, T. Lippert and K. Schilling, Int. J. Mod. Phys. C **5** (1994) 1073 [arXiv:hep-lat/9404013].
- [27] C. R. Allton, V. Gimenez, L. Giusti and F. Rapuano, Nucl. Phys. B **489** (1997) 427 [arXiv:hep-lat/9611021].